Highlight Review

Strategies for the Development of Visible-light-driven Photocatalysts for Water Splitting

Akihiko Kudo,* Hideki Kato, and Issei Tsuji

(Received August 18, 2004; CL-048011)

Abstract

Photocatalysts for water splitting developed by the present authors are reviewed. A NiO (0.2 wt %)/$NaTaO_3$:La (2%) photocatalyst with a 4.1-eV band gap showed high activity for water splitting into H_2 and O_2 with an apparent quantum yield of 56% at 270 nm. Many visible-light-driven photocatalysts have also been developed through band engineering by doping of metal cations, forming new valence bands with Bi_{6s}, Sn_{5s}, and Ag_{4d} orbitals, and by making solid solutions between ZnS with wide band gap and narrow band gap semiconductors. Overall water splitting under visible light irradiation has been achieved by construction of a Z-scheme photocatalysis system employing the visible-light-driven photocatalysts for H_2 and O_2 evolution, and the Fe^{3+}/Fe^{2+} redox couple as an electron relay.

♦ 1. Introduction

Photocatalytic reactions have been studied extensively. They are classified into two categories: uphill and downhill reactions, as shown in Figure 1. Water splitting into H_2 and O_2 is accompanied by a large positive change in the Gibbs free energy ($\Delta G^o = 237$ kJ/mol); i.e., it is an uphill reaction. In this reaction, a photon energy is converted into chemical energy, as seen in photosynthesis by green plants. Therefore, this reaction is termed artificial photosynthesis. On the other hand, degradation reactions such as the photo-oxidation of organic compounds using oxygen molecules are generally downhill reactions. The reaction proceeds irreversibly. This type of reaction is regarded as a photoinduced reaction and has been extensively studied using titanium dioxide photocatalysts.[1]

The importance of hydrogen energy has recently been re-recognized because of the interest in clean energy. Hydrogen is mainly produced by steam reforming of hydrocarbons such as methane in industry. Hydrogen must be produced from water using a renewable energy source, if one considers the energy and environmental issues. Therefore, photocatalytic water splitting is a challenging reaction because it is an ultimate solution to these serious problems.

Water splitting has been studied for a long time since the Honda–Fujishima effect, which involved a TiO_2 semiconductor electrode, was reported.[2] However, the number of reported photocatalysts that were able to decompose water into H_2 and O_2 in stoichiometric amounts with reasonable activity has been quite limited. Against such a background, various types of new photocatalysts for water splitting have recently been found,[3–5] and this research field is taking a new turn. In the present paper, new photocatalyst materials, developed mainly by the present authors and aimed at water splitting by means of artificial photosynthesis, are reviewed.

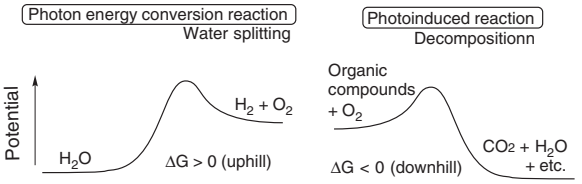

Figure 1. Types of photocatalytic reactions.

♦ 2. Processes on Photocatalytic Reactions

Figure 2 shows the main processes in a photocatalytic reaction. The first step (i) of the photocatalytic reaction is absorption of photons to form electron-hole pairs. The band gap (BG) of a visible-light-driven photocatalyst should be narrower than 3.0 eV ($\lambda > 420$ nm). Moreover, the conduction and valence band positions should satisfy the energy requirements set by the reduction and oxidation potentials for H_2O, respectively. Therefore, band engineering is necessary for the design of photocatalysts with these properties.

The second step (ii) consists of a charge separation and the migration of photogenerated carriers. The crystal structure and the crystallinity strongly affect these processes. The higher the crystalline quality, the smaller is the amount of defects. The defects operate as trapping and recombination centers between photogenerated electrons and holes, resulting in a decrease in the photocatalytic activity. Therefore, a high degree of crystallinity, rather than a high surface area, is required of photocatalysts, especially for an uphill reaction like water splitting.

The final step (iii) consists of the surface chemical reactions. The important points for this step are surface character (active sites) and quantity (surface area). Cocatalysts such as Pt, NiO, and RuO_2 are usually loaded to introduce active sites for H_2 evolution because the conduction band levels of many oxide photocatalysts are not high enough to reduce H_2O to produce H_2 without catalytic assistance. Active sites for 4-electron oxidation of H_2O are required for O_2 evolution. Although this reaction is demanding, cocatalysts are unnecessary for oxide photocata-

Prof. Akihiko Kudo,[†,††] *Dr. Hideki Kato,*[†] *and Mr. Issei Tsuji*[†]
[†]*Department of Applied Chemistry, Faculty of Science, Science University of Tokyo, 1-3 Kagurazaka, Shinjuku-ku, Tokyo 162-8601*
[††]*Core Research for Evolutional Science and Technology (CREST), Japan Science and Technology Agency (JST)*
E-mail: a-kudo@rs.kagu.tus.ac.jp

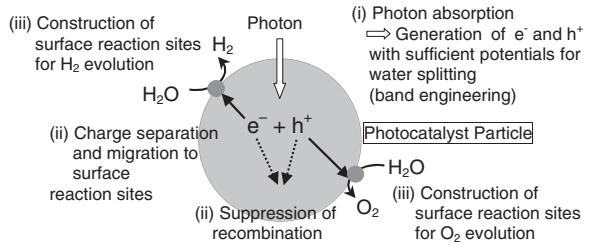

Figure 2. Processes in photocatalytic reactions.

lysts because the valence band is deep enough to oxidize H_2O to form O_2.

Many photocatalysts are also materials for solar cells, phosphors, and dielectrics. However, the significant difference between the photocatalytic property and the other properties is that chemical reactions are involved in the photocatalytic process, but not in the other properties.

♦ 3. Highly Active Tantalate Photocatalysts for Overall Water Splitting under UV Irradiation

Before presenting visible-light-driven photocatalysts, we will introduce the highly active photocatalysts for water splitting into H_2 and O_2 under UV irradiation.

We have surveyed new photocatalyst materials by paying attention to the crystal structure. Table 1 shows water splitting on various tantalate photocatalysts.[6–11] These tantalate photocatalysts were active even without cocatalysts. Moreover, loading a NiO cocatalyst drastically improved the photocatalytic performance. The conduction and valence bands of these tantalate photocatalysts consist of Ta_{5d} and O_{2p} orbitals, respectively. The conduction band level is sufficiently higher than the reduction potential of H_2O. The band position changes with the distortion as well as the mode of connection of the TaO_6 units. These tantalate photocatalysts consist of corner-shared TaO_6 octahedra in their crystal structures. A study on the luminescent properties has concluded that the closer the M–O–M bond angle is to 180°, the more the excitation energy is delocalized.[12] This tendency indicates that photogenerated electron-hole pairs can migrate relatively easily in the corner-shared framework of TaO_6 units. The present authors have applied this rule to the factors that affect photocatalytic performance.[8,10] The mobility of the electron-hole pair affects the photocatalytic activity as well as the conduction band level because it affects the probability of electrons and holes to reach reaction sites on the surface; this is an important process, as shown in step (ii) in Figure 2.

These tantalate photocatalysts were also active for the reduction of nitrate ions to N_2.[13] $NiO/KTaO_3$:Zr,[14] $NiO/RbLaTa_2O_7$,[15] and $H_2SrTa_2O_7$[16] have been reported as tantalate photocatalysts for water splitting.

$NiO/NaTaO_3$ was the most active, as shown in Table 1. The photocatalytic activity of $NiO/NaTaO_3$ increased remarkably with doping of lanthanoid ions.[17] An optimized NiO (0.2 wt %)/$NaTaO_3$:La (2%) photocatalyst showed high activity, with an apparent quantum yield of 56% for water splitting. Under irradiation of the light from a 400-W high pressure mercury lamp, H_2 and O_2 evolved at rates of 19.8 and 9.7 mmol h^{-1}, respectively, as shown in Figure 3. Gas evolution in the form of bubbles was actually observed. The activity was stable for more than 400 h.

Table 1. Water splitting on alkali metal and alkaline earth tantalate photocatalysts

Catalyst	BG / eV	NiO / mass%	Activity / μmol h^{-1}		Ref
			H_2	O_2	
$K_3Ta_3Si_2O_{13}$	4.1	none	53	23	7
$K_3Ta_3Si_2O_{13}$	4.1	1.3	390	200	7
$LiTaO_3$	4.7	none	430	220	8
$LiTaO_3$	4.7	0.1	98	52	8
$NaTaO_3$	4.0	none	160	86	8
$NaTaO_3$	4.0	0.05	2180	1100	8
$KTaO_3$	3.6	none	29	13	8
$KTaO_3$	3.6	0.05	7	3	8
$CaTa_2O_6$	4.0	none	21	8	8
$CaTa_2O_6$	4.0	0.1	72	32	8
$SrTa_2O_6$	4.4	none	140	66	9
$SrTa_2O_6$	4.4	0.1	960	490	9
$BaTa_2O_6$	4.1	none	33	15	8
$BaTa_2O_6$	4.1	0.3	629	303	8
$Sr_2Ta_2O_7$	4.6	none	53	18	10
$Sr_2Ta_2O_7$	4.6	0.15	1000	480	10
$K_2PrTa_5O_{15}$	3.8	none	10	3	11
$K_2PrTa_5O_{15}$	3.8	0.1	1550	830	11

Alkali metal tantalates were prepared in the presence of excess amounts (5%) of alkali metal.
Photocatalyst: 1.0 g; water: 390 mL; reaction cell: inner irradiation-type reaction cell made of quartz; light source: 400-W high pressure mercury lamp.

The reaction scheme for the water splitting on the $NiO/NaTaO_3$:La photocatalyst was clarified by nanoscale characterization, as shown in Figure 4. Electron microscope observations revealed that the particle size of the $NaTaO_3$:La crystal (0.1–0.7 μm) was smaller than that of the nondoped $NaTaO_3$ crystal (2–3 μm) and that the ordered surface nanosteps were created by lanthanum doping. The small particle size with high crystallinity was advantageous in terms of increasing the probability of the reactions of photogenerated electrons and holes with water molecules, rather than recombination. Transmission electron microscope observations and extended X-ray absorption fine structure analyses indicated that the NiO cocatalyst was loaded as ultra-fine NiO particles on the edges of the nanostep structures. The H_2 evolution site of the edge was effectively separated from the O_2 evolution site of the groove at the surface nanostep structure. This separation is advantageous, especially for water splitting in order to avoid the back reaction. Doping of Ca, Sr, and Ba

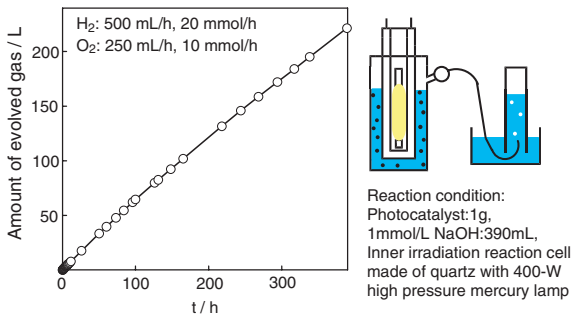

Figure 3. Total gas evolution from water on the $NiO/NaTaO_3$:La photocatalyst under UV irradiation.

Published on the web (Advance View) October 30, 2004; DOI 10.1246/cl.2004.1534

also produced the same effect as that of La on the formation of the characteristic morphology of $NaTaO_3$ and the improvement of photocatalytic performance.[18] The dynamics of photogenerated electrons in the $NaTaO_3$ photocatalyst have been studied by time-resolved IR measurements.[19]

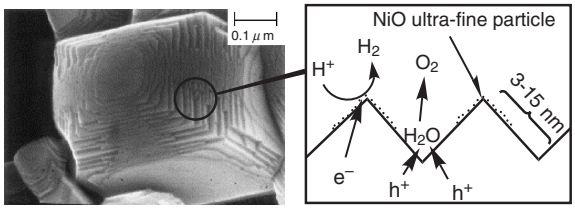

Figure 4. Mechanism of water splitting on a surface nanostep of the $NiO/NaTaO_3$:La photocatalyst.

Niobates such as $NiO/Sr_2Nb_2O_7$[10,20] and $NiO/ZnNb_2O_6$,[21] which belong to the same group as the tantalates, were also active for water splitting, although the loading of the NiO cocatalyst and pretreatment for its activation were indispensable. The difference in the photocatalytic properties between the tantalates and the niobates is mainly due to the conduction band levels. The conduction band energy associated with Ta_{5d} is higher than that associated with Nb_{4d} in the same crystal structure.[10]

♦ 4. Visible-light-driven Photocatalysts for H_2 or O_2 Evolution Developed by Band Engineering

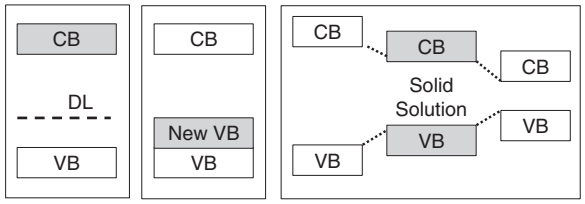

Figure 5. Three types of band engineering for the design of visible-light-driven photocatalysts.

Suitable band engineering is needed in order to develop new photocatalysts for water splitting under visible light irradiation, as mentioned in Section 2. The strategies are shown in Figure 5. In general, the conduction bands of stable oxide semiconductor photocatalysts are usually based on the metal cations with d^0 and d^{10} configurations, and consist of the empty orbitals (LUMOs) of their metal cations.[10,22] The conduction band (CB) level should be higher than the reduction potential of H_2O, i.e., that to produce H_2 ($E^o = 0$ V). On the other hand, the potential of the valence band (VB), based on O_{2p} orbitals (ca. +3 eV), is considerably more positive than the oxidation potential of H_2O, i.e., that to produce O_2 ($E^o = 1.23$ V). Therefore, the band gaps of oxide semiconductor photocatalysts inevitably become wider than the minimum necessary for water splitting. Accordingly, a new valence band or an electron donor level (DL) must be formed with orbitals of elements other than O_{2p} to make the band gap (BG) or the energy gap (EG) narrower. Making a solid solution is also a useful band engineering stratagem. We have developed visible-light-driven photocatalysts according to these strategies, as shown in Table 2.[23–36] The activities of well-known Pt/CdS and WO_3 photocatalysts are also indicated as references. These reactions were carried out in the presence of sacrificial reagents. These reactions are regarded as half-reactions for water splitting and are often employed in test reactions of photocatalytic H_2 or O_2 evolution.

Table 2. Visible-light-driven photocatalysts for H_2 or O_2 volution from aqueous solutions in the presence of sacrificial reagents

Catalyst	BG (EG) / eV	Sacrificial reagent	Activity / μmol h^{-1}		Ref
			H_2	O_2	
Pt/CdS	2.4	K_2SO_3	850	—	
WO_3	2.8	$AgNO_3$	—	65	
$Pt/SrTiO_3$:Cr,Sb	2.4	CH_3OH	78	—	23
$Pt/SrTiO_3$:Cr,Ta	2.3	CH_3OH	70	—	24
TiO_2:Cr,Sb	2.5	$AgNO_3$	—	42	23
$Pt/SrTiO_3$:Rh	2.3	CH_3OH	117	—	25
ZnS:Cu	2.5	K_2SO_3	450	—	26
ZnS:Ni	2.3	$Na_2S+K_2SO_3$	280	—	27
ZnS:Pb, Cl	2.3	$Na_2S+K_2SO_3$	40	—	28
$Pt/SnNb_2O_6$	2.3	CH_3OH	20	—	29
$BiVO_4$	2.4	$AgNO_3$	—	421	30
$AgNbO_3$	2.86	$AgNO_3$	—	37	31
Ag_3VO_4	2.0	$AgNO_3$	—	17	32
Bi_2WO_4	2.8	$AgNO_3$	—	3	33
$Pt/AgInZn_7S_9$	2.4	$Na_2S+K_2SO_3$	940	—	34
$Pt/NaInS_2$	2.3	K_2SO_3	470	—	35
$In_2O_3(ZnO)_3$	2.6	$AgNO_3$	—	1.3	36
$Pt/In_2O_3(ZnO)_3$	2.6	CH_3OH	1.1	—	36

Light source: 300-W Xe lamp; $\lambda > 420$ nm.

4.1. Transition Metal-doped Photocatalysts

The authors have paid attention to $SrTiO_3$ and ZnS as host photocatalysts, in addition to TiO_2. $Pt/SrTiO_3$ codoped with a combination of either antimony or tantalum and chromium evolved H_2 from an aqueous methanol solution under visible light irradiation ($\lambda > 420$ nm).[23,24] The codoping of antimony was also effective for a TiO_2 photocatalyst doped with chromium for O_2 evolution from an aqueous silver nitrate solution, whereas TiO_2 doped with chromium alone showed no photocatalytic activity. These photocatalysts showed absorption bands in the visible light region, as shown in Figure 6. The energy gap (EG) transition, not the band gap (BG) transition, from the donor level (DL) formed by Cr^{3+} to the conduction bands (CBs) of $SrTiO_3$ and TiO_2 corresponds to the visible light absorption. The charge balance was maintained by codoping of Sb^{5+} and Ta^{5+}, resulting in the suppression of the formation of Cr^{6+} ions and oxygen defects in the lattice.

Rh-doped $SrTiO_3$ loaded with a Pt cocatalyst produced H_2 from an aqueous methanol solution with a quantum yield of 5.2% at 420 nm.[25] The visible light response was due to the transition from the electron donor level formed by the Rh ions to the conduction band composed of the Ti_{3d} orbitals of $SrTiO_3$. This is a novel oxide photocatalyst that is active for H_2 evolution under visible light irradiation.

Cu- and Ni-doped ZnS powders[26,27] ($Zn_{0.957}Cu_{0.043}S$ and $Zn_{0.999}Ni_{0.001}S$) showed photocatalytic activities for H_2 evolution from aqueous potassium sulfite and sodium sulfide solutions. ZnS codoped with Pb and Cl was also active for H_2 evo-

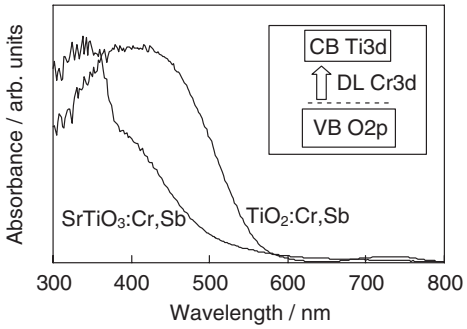

Figure 6. Diffuse reflection spectra of $SrTiO_3$ and TiO_2 photocatalysts codoped with Cr and Sb.

lution.[28] It is noteworthy that these photocatalysts showed high activities without cocatalysts such as platinum. This means that these photocatalysts possess active catalytic sites and sufficiently high conduction band levels for H_2O reduction to produce H_2, as well as a non-doped zinc sulfide photocatalyst.[37] The $Zn_{0.999}Ni_{0.001}S$ photocatalyst was also active for the reduction of nitrate and nitrite ions under visible light irradiation in the presence of a sacrificial reagent.[38]

These dopants are replacements at metal cation sites. Therefore, doping here means lattice substitution. Doping is regarded as an unsuitable method because, in most cases, the dopant works as a recombination center between photogenerated electrons and holes. However, these results indicate that doping is a suitable method, if good combinations of hosts and dopants are chosen. Recently, N- and S-doped TiO_2 powders have been studied extensively as visible-light-driven photocatalysts for decomposition reactions.[39,40]

4.2. *Valence Band-controlled Photocatalysts*

The formation of a recombination center is not completely suppressed in the doping system mentioned above. The absorption coefficient should depend on the amount of the dopant. Moreover, the impurity level formed by the doping is usually discrete and is inconvenient for the migration of photogenerated holes in that level. Therefore, a continuous valence band should be formed with some orbitals besides O_{2p}. Here, Bi^{3+} and Sn^{2+}, with ns^2 configurations, and Ag^+, with a d^{10} configuration, attracted our attention as candidates that can form such valence bands.

$SnNb_2O_6$ is a novel oxide photocatalyst for H_2 evolution, as is $SrTiO_3$:Rh.[29] $BiVO_4$, with a scheelite (monoclinic) structure,[30] $AgNbO_3$, with a perovskite structure,[31] and Ag_3VO_4[32] possessed photocatalytic activities for O_2 evolution from aqueous silver nitrate solutions under visible light irradiation ($\lambda > 420$ nm). The photocatalytic activity of $BiVO_4$ was much higher than that of commercial WO_3 with a 2.8-eV band gap, which is a well-known photocatalyst for O_2 evolution reaction under visible light irradiation.[41] The $BiVO_4$ and $AgNbO_3$ photocatalysts were also active for the decomposition of the endocrine disrupter 4-nonylphenol under visible light irradiation.[42] The $BiVO_4$ photocatalyst was synthesized by simply stirring a vanadate powder such as $K_3V_5O_{14}$ with $Bi(NO_3)_3 \cdot 5H_2O$ powder as a dispersion in water at room temperature for 3 days, as shown in Figure 7. The photocatalytic activity of the scheelite $BiVO_4$ prepared by the aqueous process was much higher than that of $BiVO_4$ prepared by a conventional solid-state reaction, even in

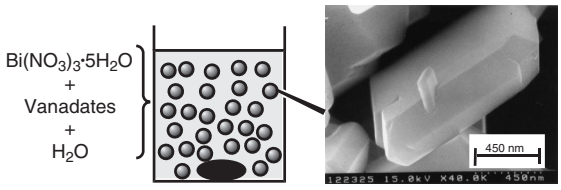

Figure 7. Synthesis of $BiVO_4$ photocatalyst at room temperature and ambient pressure in aqueous media.

the same crystal structure.[30]

These valence band-controlled photocatalysts possessed steep absorption edges in the visible light region, as shown in Figure 8, being different from the bands consisting of impurity levels, as shown in Figure 6. The steep edges indicate that the visible light absorption is due to a band–band transition. The valence bands of $BiVO_4$, $SnNb_2O_6$, and $AgNbO_3$ consist of the Bi_{6s}, Sn_{5s}, and Ag_{4d} orbitals, respectively, mixed with O_{2p}, resulting in a raising of the valence band levels and a decrease in the band gaps. It was confirmed that Ag^+ and Bi^{3+} were also effective in decreasing the band gaps of AMO_4 (M = Mo and W) photocatalysts with scheelite structures, although these photocatalysts responded to only UV.[43] Bi_2WO_4, with the Aurivillius structure, was also active for O_2 evolution.[33]

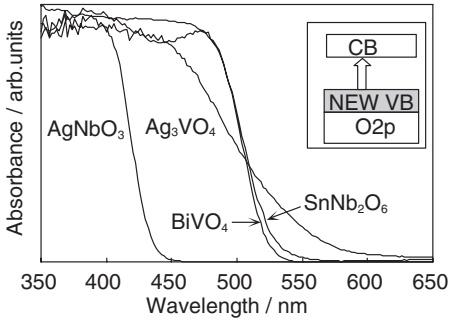

Figure 8. Diffuse reflection spectra of valence band-controlled photocatalysts containing of Bi, Sn, and Ag.

N_{2p} and S_{3p} are also suitable orbitals to form valence bands, as seen in nitride, oxynitride, and oxysulfide photocatalysts with visible light response.[44]

4.3. *Solid Solution Photocatalysts*

Although metal sulfides always have a problem of photocorrosion, they are attractive as photocatalysts with visible light response. A representative photocatalyst is Pt/CdS which is active for H_2 evolution under visible light irradiation. The photocorrosion is considerably suppressed in the presence of sacrificial reagents. ZnS is an interesting photocatalyst material from the viewpoint of its preeminent ability to produce H_2,[37] as confirmed for Cu- and Ni-doped ZnS. ZnS is able to form $(AgIn)_xZn_{2(1-x)}S_2$ solid solutions with a narrow band gap semiconductor, $AgInS_2$.[45] The solid solutions include Ag, which is expected to contribute to valence band formation, as observed for an $AgNbO_3$ photocatalyst.[31] $(AgIn)_xZn_{2(1-x)}S_2$ solid solutions showed photocatalytic activities for H_2 evolution from aqueous solutions containing sacrificial reagents, SO_3^{2-} and S^{2-}, under visible light irradiation ($\lambda > 420$ nm) even without Pt cocatalysts.[34] Loading of the Pt cocatalyst improved the photocatalytic activity. Pt (3 wt %)-loaded $(AgIn)_{0.22}Zn_{1.56}S_2$, with a 2.3-eV

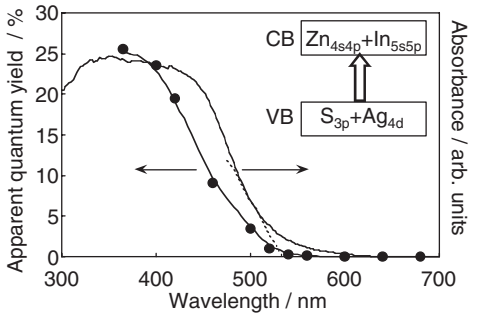

Figure 9. Action spectrum for H_2 evolution on the $(AgIn)_{0.22}$-$Zn_{1.56}S_2$ solid solution photocatalyst.

band gap, showed the highest activity for H_2 evolution and the apparent quantum yield at 420 nm amounted to 20%. H_2 gas evolved at a rate of 3.3 L m^{-2} h^{-1} under irradiation using a solar simulator (AM 1.5). $M^IM^{III}S_2$ (M^I: Ag and Cu, M^{III}: Ga and In) and their solid solutions were also active for H_2 evolution. $NaInS_2$ was also found to be a unique sulfide photocatalyst with a layered structure.[35]

It is important to see the action spectrum in order to evaluate a visible-light-driven photocatalyst. The onset of the action spectrum of the $(AgIn)_{0.22}Zn_{1.56}S_2$ photocatalyst agreed with the absorption edge, indicating that the reaction proceeded photocatalytically via the band gap transition from the valence band, consisting of S_{3p} and Ag_{4d} orbitals, to the conduction band, consisting of Zn_{4s4p} and In_{5s5p} orbitals, as shown in Figure 9. It was found from SEM and TEM observations that the solid solutions partly had surface nanostep structures on their surfaces. Pt cocatalysts were selectively photodeposited as nano-dots or nanobeads on the edges of the surface nanosteps. The specific surface nanostructure was effective for the suppression of recombination between photogenerated electrons and holes, and the separation of H_2 evolution sites from oxidation reaction sites, as with the $NiO/NaTaO_3$:La photocatalyst.

These sulfide photocatalysts that show high activities for H_2 evolution are expected to turn into a practical application for H_2 production using by-products such as hydrogen sulfide emitted from the hydrogenated desulfurization process at petrochemical plants and in the mining industries.

Nb_2O_5–Bi_2O_3,[46] Ga_2O_3–In_2O_3,[47] $Sr_2Nb_2O_7$–$Sr_2Ta_2O_7$,[48] SnO_2–TiO_2,[49] ZnS–CdS,[50] and CdS–CdSe[51] solid solution photocatalysts have been reported, and their photophysical properties and photocatalytic activities are dependent on their compositions.

♦ 5. Overall Water Splitting under Visible Light Irradiation by a Two-photon Process

Sayama, Arakawa, and co-workers reported overall water splitting by the Z-scheme for a system that consisted of a Pt/$SrTiO_3$:Cr,Ta photocatalyst for H_2 evolution,[24] a WO_3 photocatalyst for O_2 evolution,[41] and the IO_3^-/I^- redox couple.[52] This system gave an apparent quantum yield of 0.1% and responded to 450 nm, which was limited by the band gap of WO_3.

We have evaluated the visible-light-driven photocatalysts listed in Table 2 for the construction of Z-scheme photocatalysis systems. Pt/$SrTiO_3$:Rh functioned as a photocatalyst for H_2 production using Fe^{2+} ions, while $BiVO_4$ and Bi_2MoO_6 were active photocatalysts for O_2 production using Fe^{3+} ions. Thus, overall water splitting under visible light irradiation has been achieved by using these photocatalysts, which possess activity for the half-reactions of water splitting and the Fe^{3+}/Fe^{2+} redox couple, as shown in Figure 10.[53] The apparent quantum yields of the (Pt/$SrTiO_3$:Rh)–($BiVO_4$), –(Bi_2MoO_6), and –(WO_3) systems were 0.3, 0.2, and 0.2%, respectively, at 440 nm. The (Pt/$SrTiO_3$:Rh)–($BiVO_4$) system responded to visible light up to 520 nm.

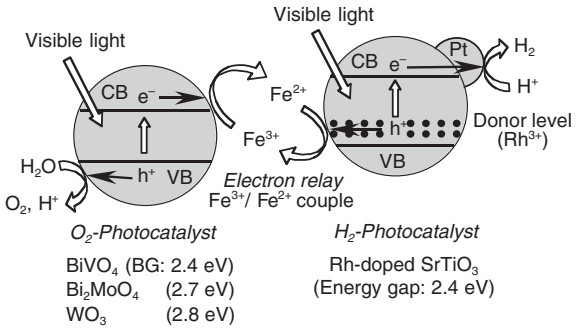

Figure 10. Water splitting system by a two-photon process with visible light response.

♦ 6. Summary and Outlook

$NiO/NaTaO_3$:La was found to be a highly active photocatalyst for water splitting, a very demanding reaction, under UV light irradiation. This result has proven that highly efficient water splitting is actually possible using a particulate photocatalyst system. Moreover, although sacrificial reagents are needed, various oxide and sulfide photocatalysts for H_2 or O_2 evolution under visible light irradiation have been developed. Efficient H_2 evolution was demonstrated for the sulfide solid solution photocatalysts with a solar simulator (AM 1.5). Overall water splitting has been accomplished by constructing systems involving the two-photon process, combining photocatalysts developed by the present authors.

It is said that the target for photocatalytic water splitting is to develop photocatalysts with a 2-eV band gap and a 30% quantum yield. There is still a difficult barrier to surmount in order to accomplish this target. The present authors believe that it is important to develop a library of photocatalyst materials. This work will clarify the factors dominating photocatalytic properties and give information for the design of highly active photocatalysts. Continuing this research will lead us to find highly active photocatalyst systems for H_2 production from water using solar light energy to achieve artificial photosynthesis.

♦ Acknowledgements

This work was partly supported by a Grant-in-Aid for Scientific Research on Priority Areas (417) from the Ministry of Education, Culture, Sports, Science and Technology of the Japanese Government. Professor Kobayashi of Kurashiki University of Science and the Arts is acknowledged for his help with the DFT calculations.

References

1 A. Fujishima, T. N. Rao, and D. A. Tryk, *J. Photochem. Photobiol., C*, **1**, 1 (2000).

2 A. Fujishima and K. Honda, *Nature*, **238**, 37 (1972).
3 A. Kudo, *Hyomen*, **36**, 625 (1998).
4 K. Domen, J. N. Kondo, M. Hara, and T. Takata, *Bull. Chem. Soc. Jpn.*, **73**, 1307 (2000).
5 A. Kudo, *Catal. Surv. Asia*, **7**, 31 (2003).
6 H. Kato and A. Kudo, *Catal. Today*, **78**, 561 (2003).
7 A. Kudo and H. Kato, *Chem. Lett.*, **1997**, 867.
8 a) H. Kato and A. Kudo, *Chem. Phys. Lett.*, **295**, 487 (1998). b) H. Kato and A. Kudo, *Catal. Lett.*, **58**, 153 (1999). c) H. Kato and A. Kudo, *J. Phys. Chem. B*, **105**, 4285 (2001).
9 H. Kato and A. Kudo, *Chem. Lett.*, **1999**, 1207.
10 A. Kudo, H. Kato, and S. Nakagawa, *J. Phys. Chem. B*, **104**, 571 (2000).
11 A. Kudo, H. Okutomi, and H. Kato, *Chem. Lett.*, **2000**, 1212.
12 a) G. Blasse and L. H. Brixner, *Mater. Res. Bull.*, **24**, 363 (1989). b) G. Blasse, *J. Solid State Chem.*, **72**, 72 (1988). c) A. M. Srivastava and J. F. Ackerman, *J. Solid State Chem.*, **134**, 187 (1997).
13 H. Kato and A. Kudo, *Phys. Chem. Chem. Phys.*, **4**, 2833 (2002).
14 T. Ishihara, H. Nishiguchi, K. Fukamachi, and Y. Takita, *J. Phys. Chem. B*, **103**, 1 (1999).
15 M. Machida, K. Miyazaki, S. Natsushima, and M. Arai, *J. Mater. Chem.*, **13**, 1433 (2003).
16 K. Shimizu, Y. Tsuji, T. Hatamach, K. Toda, T. Kodama, M. Sato, and Y. Kitayama, *Phys. Chem. Chem. Phys.*, **6**, 1064 (2004).
17 a) A. Kudo and H. Kato, *Chem. Phys. Lett.*, **331**, 373 (2000). b) H. Kato, K. Asakura, and A. Kudo, *J. Am. Chem. Soc.*, **125**, 3082 (2003).
18 A. Iwase, H. Kato, and A. Kudo, *Chem. Lett.*, **33**, 1260 (2004).
19 A. Yamakata, T. Ishibashi, H. Kato, A. Kudo, and H. Onishi, *J. Phys. Chem. B*, **107**, 14383 (2003).
20 D. W. Hwang, H. G. Kim, J. Kim, K. Y. Cha, Y. G. Kim, and J. S. Lee, *J. Catal.*, **193**, 40 (2000).
21 A. Kudo, S. Nakagawa, and H. Kato, *Chem. Lett.*, **1999**, 1197.
22 a) K. Ikarashi, J. Sato, H. Kobayashi, N. Saito, H. Nishiyama, and Y. Inoue, *J. Phys. Chem. B*, **106**, 9048 (2002). b) J. Sato, N. Saito, H. Nishiyama, and Y. Inoue, *J. Phys. Chem. B*, **107**, 7965 (2003).
23 H. Kato and A. Kudo, *J. Phys. Chem. B*, **106**, 5029 (2002).
24 T. Ishii, H. Kato, and A. Kudo, *J. Photochem. Photobiol., A*, **163**, 181 (2004).
25 R. Konta, T. Ishii, H. Kato, and A. Kudo, *J. Phys. Chem. B*, **108**, 8992 (2004).
26 A. Kudo and M. Sekizawa, *Catal. Lett.*, **58**, 241 (1999).
27 A. Kudo and M. Sekizawa, *Chem. Commun.*, **2000**, 1371.
28 I. Tsuji and A. Kudo, *J. Photochem. Photobiol., A*, **156**, 249 (2003).
29 Y. Hosogi, K. Tanabe, H. Kato, H. Kobayashi, and A. Kudo, *Chem. Lett.*, **33**, 28 (2004).
30 a) A. Kudo, K. Ueda, H. Kato, and I. Mikami, *Catal. Lett.*, **53**, 229 (1998). b) A. Kudo, K. Omori, and H. Kato, *J. Am. Chem. Soc.*, **121**, 11459 (1999). c) S. Tokunaga, H. Kato, and A. Kudo, *Chem. Mater.*, **13**, 4624 (2001).
31 H. Kato, H. Kobayashi, and A. Kudo, *J. Phys. Chem. B*, **106**, 12441 (2002).
32 R. Konta, H. Kato, H. Kobayashi, and A. Kudo, *Phys. Chem. Chem. Phys.*, **5**, 3061 (2003).
33 A. Kudo and S. Hijii, *Chem. Lett.*, **1999**, 1103.
34 a) A. Kudo, I. Tsuji, and H. Kato, *Chem. Commum.*, **2002**, 1958. b) I. Tsuji, H. Kato, H. Kobayashi, and A. Kudo, *J. Am. Chem. Soc.*, in press.
35 A. Kudo, A. Nagane, I. Tsuji, and H. Kato, *Chem. Lett.*, **2002**, 882.
36 A. Kudo and I. Mikami, *Chem. Lett.*, **1998**, 1027.
37 J. F. Reber and K. Meier, *J. Phys. Chem.*, **88**, 5903 (1984).
38 O. Hamanoi and A. Kudo, *Chem. Lett.*, **2002**, 838.
39 R. Asahi, T. Morikawa, T. Ohwaki, K. Aoki, and Y. Tagaya, *Science*, **293**, 269 (2001).
40 T. Ohno, T. Mitsui, and M. Matsumura, *Chem. Lett.*, **32**, 364 (2003).
41 J. R. Darwent and A. Mills, *J. Chem. Soc., Faraday. Trans. 2*, **78**, 359 (1982).
42 a) S. Kohtani, S. Makino, A. Kudo, K. Tokumura, Y. Ishigaki, T. Matsunaga, O. Nikaido, K. Hayakawa, and R. Nakagaki, *Chem. Lett.*, **2002**, 660. b) S. Kohtani, M. Koshiko, A. Kudo, K. Tokumura, Y. Ishigaki, A. Toriba, K. Hayakawa, and R. Nakagaki, *Appl. Catal., B*, **46**, 573 (2003). c) S. Kohtani, N. Yamamoto, K. Kitajima, A. Kudo, H. Kato, K. Tokumura, K. Hayakawa, and R. Nakagaki, *Photo/Electrochem. Photobiol. Environ. Energy and Fuel*, **2004**, 173.
43 H. Kato, N. Matsudo, and A. Kudo, *Chem. Lett.*, **33**, 1216 (2004).
44 a) M. Hara, G. Hitoki, T. Takata, J. N. Kondo, H. Kobayashi, and K. Domen, *Stud. Surf. Sci. Catal.*, **145**, 169 (2003). b) M. Hara, G. Hitoki, T. Takata, J. N. Kondo, H. Kobayashi, and K. Domen, *Catal. Today*, **78**, 555 (2003). c) A. Kasahara, N. Nukumizu, T. Takata, J. N. Kondo, M. Hara, H. Kobayash, and K. Domen, *J. Phys. Chem. B*, **107**, 791 (2003). d) A. Ishikawa, T. Takata, J. N. Kondo, M. Hara, H. Kobayashi, and K. Domen, *J. Am. Chem. Soc.*, **124**, 13547 (2002).
45 a) V. G. Lambrecht, *Mater. Res. Bull.*, **7**, 1411 (1972). b) I. D. Olekseyuk, V. O. Halka, O. V. Parasyuk, and S. V. Voronyuk, *J. Alloys Compd.*, **325**, 204 (2001).
46 A. Harriman, J. M. Thomas, W. Zhou, and D. A. Jefferson, *J. Solid State Chem.*, **72**, 126 (1988).
47 A. Kudo and I. Mikami, *J. Chem. Soc., Faraday Trans.*, **94**, 2929 (1998).
48 a) H. Kato and A. Kudo, *J. Photochem. Photobiol., A*, **145**, 129 (2001). b) M. Yoshino, M. Kakihana, W. S. Cho, H. Kato, and A. Kudo, *Chem. Mater.*, **14**, 3369 (2002).
49 J. Lin, J. C. Yu, D. Lo, and S. K. Lam, *J. Catal.*, **183**, 368 (1999).
50 a) H. C. Youn, S. Baral, and J. H. Fendler, *J. Phys. Chem.*, **92**, 6320 (1988). b) H. Inoue, H. Moriwaki, K. Maeda, and H. Yoneyama, *J. Photochem. Photobiol., A*, **86**, 191 (1995).
51 a) S. Kambe, M. Fujii, T. Kawai, and S. Kawai, *Chem. Phys. Lett.*, **109**, 105 (1984). b) T. Uchihara, H. Abe, M. Matsumura, and H. Tsubomura, *Bull. Chem. Soc. Jpn.*, **62**, 1042 (1989).
52 K. Sayama, K. Mukasa, R. Abe, Y. Abe, and H. Arakawa, *Chem. Commun.*, **2001**, 2416.
53 H. Kato, M. Hori, R. Konta, Y. Shimodaira, and A. Kudo, *Chem. Lett.*, **33**, 1348 (2004).